Enhancement of Trabecular Bone on Dental Panoramic Radiographs Using Multiscale Line Operator

Agus Zainal Arifin, Dwi Izzatul Millah, Imam Cholissodin, and Indra Lukmana
Vision and Image Processing Laboratory, Department of Informatics, Faculty of Information Technology, Institut Teknologi Sepuluh Nopember (ITS), Surabaya, 60111, Indonesia

E-mail: agusza@cs.its.ac.id, di.millah@cs.its.ac.id, imam09@cs.its.ac.id, indra_801@cs.its.ac.id

Abstract - Mandibular bone on dental panoramic radiographs provides information that can be used to diagnose several diseases. One of the most complex structures inside is trabecular bone. Manual analysis on the trabecular bone structure, however, is very difficult. This paper discussed a method to clarify and sharpen the structure of the trabecular bone on dental panoramic radiographs which will give a better medical information and easier to be analyzed. We employed multi-scale line operators (MSLO) to detect the linear structure on trabecular bone in dental panoramic radiographs. Our experiment achieved the highest average of 16109 white pixels from 15 dental panoramic radiographs.
Keywords: blood-vessel segmentation; multiscale line operators.

I. INTRODUCTION

The detection of trabecular bone linear structure is an important task because it provides information that can be used to diagnose several diseases including osteoporosis. The linear structures of trabecular bone are almost similar with retinal blood vessel which has various widths. Several methods of segmentation have been proposed including locally adaptive schemes, pattern recognition (multiscale approaches, skeletons, region growing, ridge-based approaches, blood-vessel tracking, matched filter, differential geometry, and mathematical morphology), model-based approaches e.g. active snakes, and artificial intelligence and neural networks [1–23].

Some algorithms have been already developed for detecting and tracing retinal blood vessels even for this relatively small branch of medical image processing [2–23]. One of the simplest approaches that one can employ in order to segment blood vessels is to use adaptive thresholding [4–6]. Adaptive thresholding chooses the threshold independently at each pixel based on local or global information. For example, the mean or median grayscale value in some locale around a given pixel is used as the threshold at this pixel. This is repeated for all pixels in order to produce a binary image that we shall refer to as the vessel segmentation. Another relatively straightforward method that has been used to enhance vessel segmentation is edge detection [7].

More sophisticated approaches have also been used to segment blood vessels in retinal images [8–20]. Such approaches often use information about the expected properties of blood vessels in digital fundus images in order to enhance vessel segmentation. This might be, for example, that the vessels are roughly piecewise linear and that their cross sectional profiles are approximately Gaussian. One method that has been employed often and with great success is that of two-dimensional matched filter such as Gaussian profiles [8] that have a particular direction and width in the two- dimensional plane of the image [8–13]. Subsequent adaptive threshold probing of a matched filter response has also been employed [13] in order to track blood vessels with much success. Mathematical morphology with curvature estimation [14, 15] and ridge-based vessel segmentation procedures [15, 16] have also been used to segment blood vessels in fundus images. Some approaches exploit the expected cross-sectional profiles of blood vessels which form centerlines form ridges in the grayscale topology of the image [14–19]. Another interesting approach used fuzzy clustering in order segment blood vessels [22]. Line operators and support vector classification have also been employed with much success [23]. The methods presented in Refs. [12–23] are sophisticated and they represent the state- of-art for vessel segmentation at the moment. A research which combine many of these approaches is by utilizing image information at a variety of length scales [21,22].

A relatively straightforward multiscale approach is provided by the multiscale line operator (MSLO) [24–30]. In previous researches, implementation of multiscale line operator algorithm was used to detect asbestos fiber [24] also In [25], this algorithm is applied to detect linear structure of iris blood vessel. This method has been used with great success in detecting linear structures in mammograms [26–30].

Dental panoramic radiographs generally contain linear structures of trabecular bone of varying widths. Hence, the application of a filter of fixed width and at only one length scale would necessarily bias the procedure towards linear structures of trabecular bone of a similar width. Multiscale techniques are thus often employed in linear structures of trabecular bone detection in order to overcome this problem.

In the context of linear structures of trabecular bone detection, MSLO expected to work well. Furthermore,

linear structures of trabecular bone of varying width are treated, in principle, on an equal footing. This approach also has the additional advantage of being conceptually simple.

In this paper we propose a method to clarify and sharpen the structure of the trabecular bone on dental panoramic radiographs which will give a better medical information and easier to be analyzed using MSLO.

II. METHOD

We now present explanations of the algorithms to delineate linear structures of trabecular bone in dental panoramic radiographs.

A. Multiscale Line Operator

MSLO is used in order to detect the linear structures of trabecular bone in the image. For each pixel in the original image at point (i, j), the mean average value, P, of the grayscale values of line of fixed pixels centered on (i, j) was obtained. However, we also determined the average grayscale value, Q, of those pixels in an area or 'locale' surrounding this line. As in previous studies [24–30], the shape of the locale was taken to be a square (see Fig. 1). The response of the filter at point (i, j) of the line (at given orientation) was given by

$$S = P - Q \qquad (1)$$

This process was repeated at various orientations of the line between 0º and 180º. The largest value of S over all of these orientations was taken to be the value of the line operator at that pixel. The subtraction of the mean grayscale value of local environment Q, from the mean value for the line P, in Eq. (1) ensured that changes in background illumination were also removed from the filtered image, S. Inline with [24–30], we used a line operator of length five pixels obtained at 12 orientations only.

In Fig.1. the line operator was applied by determining the mean average value P, of the grayscale values of the pixels in shaded rectangles. The average value Q, of all other pixels indicated by the unshaded rectangles was also obtained. The response was given by S and this is repeated for 12 orientations of the line. The result for the central pixel was the largest value of S for all 12 orientations.

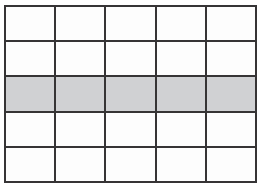

Fig.1. Line Operator

The line operator was applied at varying levels of scale by constructing a series of images at consecutively larger length scales via Gaussian sampling with respect the original 'raw' image. The resulting series of sub sampled images constructed is referred to here as a 'Gaussian pyramid'; the number of levels of the Gaussian pyramid here taken as the variables. The line operator then applied to the images on each level of the pyramid separately. The line-operator filtered images on the coarser scales of the pyramid then mapped to the original level of scale by using a cubic spline. The final result was the sum of all images in the Gaussian pyramid and equal weighting is given to each length scale in the final MSLO image. A threshold then applied to the image to form an initial binary segmentation.

III. RESULT

Result for application of MSLO applied on a dental panoramic radiographs are shown in Fig. 2, the figure shows the original grayscale dental panoramic radiographs and the results of applying the MSLO to it with three levels image pyramid. The grayscale values of the filtered image were also scaled to lie in the range [0, 255] and then 'inverted' (i.e., grayscale value 255 to 0 and 0 to 255) in order to produce an eight-bit grayscale image. The linear structures of trabecular bone can be clearly seen as the white lines in the image.

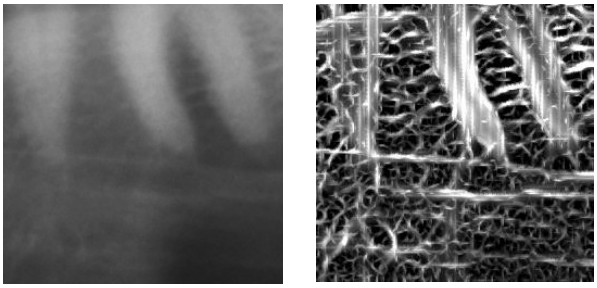

(a) (b)

Fig. 2. MSLO Application on Dental Panoramic Radiograph

TABLE I
WHITE PIXEL CALCULATION RESULTS

Image	Multiscale Line Operator		
	Level 1	Level 2	Level 3
A	10776	15806	19303
B	10097	15063	18606
C	12294	16198	18545
D	11601	16224	18291
E	10961	13264	16673
F	4886	5094	5676
G	10453	15112	18186
H	10021	14240	17496
I	7499	10119	13162
J	9378	12847	15842
K	7667	12108	14658
L	8670	12108	16263
M	11147	15967	19318
N	15285	17535	20084
O	7342	8413	9529
Average	9872	13340	16109

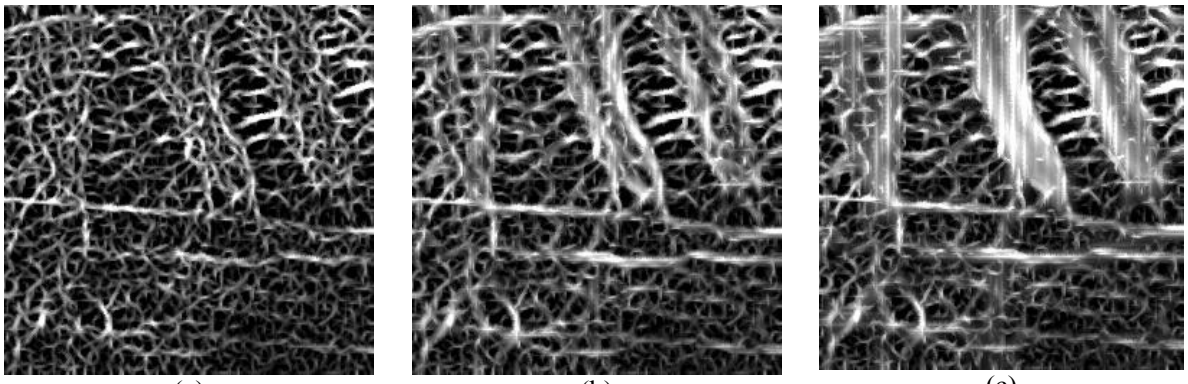

(a) (b) (c)

Fig. 3 Result Images of MSLO on Every Level.

The results for calculating white pixel for 15 processed images with every level of multiscale line operator are shown in Table 1, here we achieved the highest average of 16109 on level 3 MSLO.

Result images sample of every level of multiscale line operator are shown in Fig. 3. Fig. 3a shows the result image from applied multiscale line operator level 1, Fig. 3b shows the result image from applied multiscale line operator level 2, and Fig. 3c shows the result image from applied multiscale line operator level 3. As shown in this figure, the best results for detection of trabecular bone in dental panoramic radiographs were found by using three levels in the image pyramid.

Comparing with the similar method [31], the proposed method achieved better results in speed and enhancement quality, due to consideration of orientation and several parameter optimizations.

IV. CONCLUSION

The results of the MSLO can provide good estimation of the positions and widths of the linear structures of trabecular bone. The average of white pixel from 15 dental panoramic radiographs for the MSLO were found by using three levels in the image pyramid is 16109. By employing the line operator at different scales, the results were found to be less susceptible to noise than application of the filter at the finest level of detail only. The final response was a linear sum of responses at all length scales considered with equal weighting.

Speed is crucial to any practical real world application of automated linear structures of trabecular bone detecting at the point of image capture e.g., as a screening tool for osteoporosis. However, the accuracy of the linear structures of trabecular bone detection procedure is also affected by its complexity. Accuracy will probably affect the strength of correlations of extracted biometric parameters from the linear structures of trabecular bone detection with osteoporosis. Hence, the practical importance of the results presented in this article is that the method has been presented can produce good accuracy and fast enough to be able to be employed in the clinic.

In conclusion, we have proven in this article that the application of MSLO techniques can lead to an enhancement of linear structures of trabecular bone detection in dental panoramic radiographs. However, our results were found to be as good as previous detection linear structures of trabecular bone procedures. Our approach was found to be fast enough, in principle, to be employed at the point of image capture.

REFERENCES

[1] C. Kirbas, F.H. Quek, A review of vessel extraction techniques and algorithms, ACM Compute. Survey. 36 (2004) 81–121.

[2] M. Niemeijer, J. Staal, B. van Ginnekan, M. Long, M.D. Abramoff, Comparative study of retinal vessel segmentation methods on a new publicly available database, Proc. SPIE Med. Imaging 5370 (2004) 648–656.

[3] A. Pinz, S. Bernogger, P. Datlinger, A. Kruger, Mapping the human retina, IEEE Trans. Med. Imaging 17 (1998) 606–619.

[4] Y. Wang, S.C. Lee, A fast method for automated detection of blood vessels in retinal images, in: Proceedings of the Conference Record of the Thirty-First Asilomar Conference on Signals, Systems & Computers, vol. 2, 1997, pp. 1700–1704.

[5] X. Jiang, D. Mojon, Adaptive local thresholding by verification based multithreshold probing with application to vessel detection in retinal images, IEEE Trans. Pattern Anal. Mach. Intell. 25 (2003) 131–137.

[6] D. Wu, M. Zhang, J.-C. Liu, W. Bauman, on the adaptive detection of blood vessels in retinal images, IEEE Trans. Biomed. Eng. 53 (2006) 341–343.

[7] H. Li, O. Chutatape, Fundus image features extraction, in: Proceedings of the 22nd Annual EMBS International Conference, 2000, pp. 3071–3073.

[8] Chaudhuri, S. Chatterjee, N. Katz, M. Nelson, M. Goldbaum, Detection of blood vessels in retinal images using two dimensional matched filters, IEEE Trans. Med. Imaging 8 (1989) 263–269.

[9] O. Chutatape, L. Zeng, S. Krishman, Retinal blood vessel detection and tracking by matched Gaussian and Kalman filter, in: Proceedings of the 20th Annual International Conference of the IEEE Engineering in Medicine and Biology Society, vol. 20, 1998, pp. 3144–3149.

[10] L. Gang, O. Chutatape, S.M. Krishnan, Detection and measurement of retinal vessels in fundus images using amplitude modified second-order Gaussian filter, IEEE Trans. Biomed. Eng. 49 (2002) 168–172.

[11] H.L. Hsu, W.M.L. Lee, T.Y. Wong, Automatic grading of

retinal vessel calibre, IEEE Trans. Biomed. Eng. 52 (2005) 1352–1355.
[12] D. Satyarthi, M.R. Kumar, S. Dandapat, Gaussian intensity distribution modeling of blood vessels in fundus images, in: Proceedings of IEEE INDICON 2005 Conference, 2005, pp. 228–232.
[13] A.D. Hoover, V. Kouznetsova, M. Goldbaum, Locating blood vessels in retinal images by piecewise threshold probing of a matched filter response, IEEE Trans. Med. Imaging 19 (2000) 203–210.
[14] F. Zana, J.-C. Klein, Segmentation of vessel-like patterns using mathematical morphology and curvature evaluation, IEEE Trans. Image Process. 10 (2001) 1010–1019.
[15] A.M. Mendonc¸a, A. Campilho, Segmentation of retinal blood vessels by combining the detection of centerlines and morphological reconstruction, IEEE Trans. Med. Imaging 25 (2006) 1200–1213.
[16] M.E. Martinez-Perez, A.D. Hughes, S.A. Thom, A.A. Bharath, K.H. Parker, Segmentation of blood vessels from red-free and fluorescein retinal images, Med. Image Anal. 11 (2007) 47–61.
[17] J. Staal, M.D. Abramoff, M. Neimeijer, M.A. Viergever, B. van Ginneken, Ridge-based vessel segmentation in color images of the retina, IEEE Trans. Med. Imaging 23 (2004) 501–509.
[18] N.M. Salem, A.K. Nandi, Segmentation of retinal blood vessels using scale-space features and k-nearest- neighbor classifier, in: Proceedings of the IEEE International Conference on Acoustics, Speech, and Signal Processing, ICASSP 2006, vol. 2, 2006, pp. 1001–1004.
[19] K.A. Vermeer, F.M. Vos, H.G. Lemij, A.M. Vossepoel, A model based method for retinal blood vessel detection, Comput. Biol. Med. 34 (2004) 209–219.
[20] A. Tolias, S.M. Panas, A fuzzy vessel tracking algorithm for retinal images based on fuzzy clustering, IEEE Trans. Med. Imaging 17 (1998) 263–273.
[21] M. Martinez-Perez, A. Hughes, A. Stanton, S. Thom, A. Bharath, K. Parker, Scale-space analysis for the characterization of retinal blood vessels, in: Medical Image Computing and Computer-Assisted Intervention, MICCAI 1999, pp. 90–97.
[22] A.F. Frangi, W.J. Niessen, K.L. Vincken, M.A. Viergever, Multiscale vessel enhancement filtering in: Medical Image Computing and Computer-Assisted Intervention—MICCAI 1998, pp. 130–137.
[23] E. Ricci, R. Perfetti, Retinal blood vessel segmentation using line operators and support vector classification, IEEE Trans. Med. Imaging 26 (2007) 1357–1365.
[24] R.N. Dixon and C.J. Taylor,"Automated Asbestos Fiber Counting", ser. Conference. Philadelphia, PA: Ist.Phsics, vol. 44, pp.178-185, 1979.
[25] D.J.J Farnel, F.N Hatfield, P. Knox, M. Reakes, S. Spencer, D. Parry, S.P. Harding, "Enhancement of blood vessels in digital fundus photographs via the application of multiscale line operators", Elsivier, Vol.345, Issue 7, pp. 748-765, 15 October 2008.
[26] Zwiggelaar and C.R.M. Boggis, The benefit of knowing your linear structures in mammographic images, in: Proceedings of Medical Image Understanding and Analysis 2002, pp. 73–76.
[27] R. Zwiggelaar, T.C. Parr, C.J. Taylor, Finding orientated line patterns in digital mammographic images, in: Proceedings of the 7th British Machine Vision Conference, 1996, pp. 715–724.
[28] R. Marti, R. Zwiggelaar, C. Rubin, Automatic registration of mammograms based on linear structures, in: Information Processing in Medical Imaging, Lecture Notes in Computer Science, vol. 2082, Springer, Heidelberg, 2001, pp. 162–168.
[29] R. Zwiggelaar, S.M. Astley, C.R. Boggis, C.J. Taylor, Linear structures in mammographic images: detection and classification, IEEE Trans. Med. Imaging 23 (2004) 1077–1086.
[30] E.M. Hadley, E.R.E. Denton, R. Zwiggelaar, Mammographic risk assessment based on anatomical linear structures, in: Digital Mammography, Lecture Notes in Computer Science, vol. 4046, Springer, Heidelberg 2006.
[31] Z. Abidin and A.Z. Arifin, "Analisa Kerapatan Trabecular Bone Berbasis Graph Berbobot Pada Citra Panorama Gigi untuk Identifikasi Osteoporosis", Jurnal Ilmiah Teknologi Informasi 7 No. 2 (2008).